

Supplementary Materials for

The energy landscape of -1 ribosomal frameshifting

Junhong Choi, Sinéad O'Loughlin, John F. Atkins, Joseph D. Puglisi*

*Corresponding author. Email: puglisi@stanford.edu

Published 1 January 2020, *Sci. Adv.* 6, eaax6969 (2020)

DOI: 10.1126/sciadv.aax6969

The PDF file includes:

- Fig. S1. EF-G-bound lifetimes for translocation and mRNA structure unfolding.
- Fig. S2. Design of the frameshifting cassette and mRNA structures.
- Fig. S3. Assignment of -1 frameshifted population in smFRET assay.
- Fig. S4. Simulation of irreversible -1 frameshifting.
- Fig. S5. Western blot gel images for Fig. 5.
- Fig. S6. Internal SD sequence tilts the energy landscape of the frameshifting.
- Fig. S7. The concentration of EF-G does not alter frameshifting efficiency.
- Table S1. In vivo measurements for frameshifting constructs.
- Table S2. In vivo measurements for frameshifting on slippery sequence repeat constructs.

Other Supplementary Material for this manuscript includes the following:

(available at advances.sciencemag.org/cgi/content/full/6/1/eaax6969/DC1)

Data file S1 (Microsoft Excel format). Nucleic acid sequences for mRNA construct used in the study.

Data file S2 (Microsoft Excel format). Experimental data presented in the main and supplementary figures.

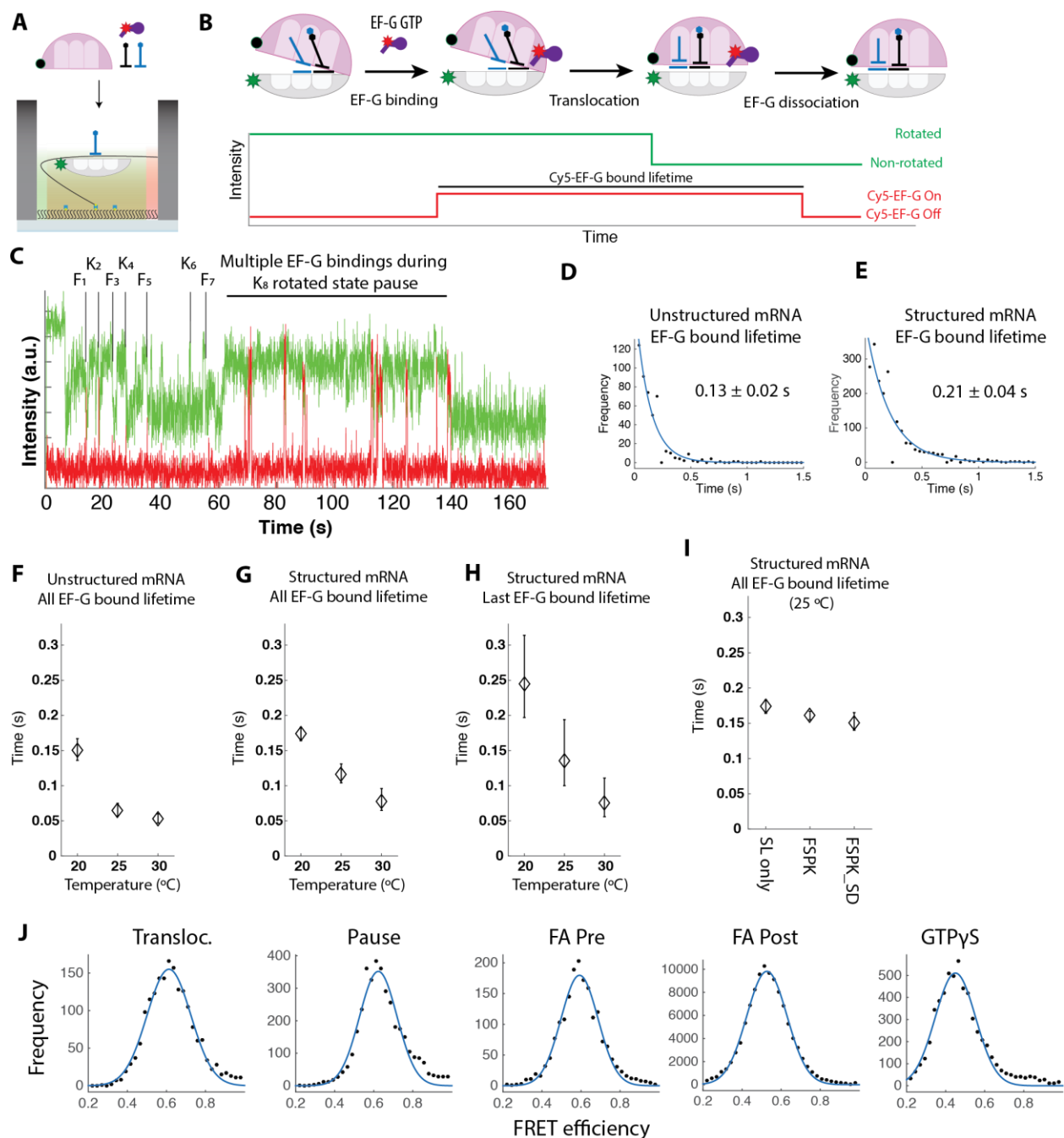


Fig. S1. EF-G-bound lifetimes for translocation and mRNA structure unfolding. (A) Schematic of single-molecule *in vitro* fluorescence assay to monitor translation dynamics using FRET donor-quencher (Cy3B and BHQ-2 pair) labeled ribosomes and Cy5-labeled EF-G. Translation pre-initiation complex (30S-PIC) containing Cy3B-labeled 30S is immobilized on the bottom of the zero-mode waveguide (ZMW) wells, and a buffer containing elongation components – BHQ-2-labeled 50S, Cy5-labeled elongation factor G (Cy5-EF-G), and tRNA – is delivered at the beginning of the experiment. (B) Conformational changes of the ribosome during translation elongation and the expected fluorescence signal. The time between two conformational changes is measured as a rotated state lifetime for each codon. (C) The representative trace shows multiple bindings of Cy5-labeled EF-G during translocation pause induced by mRNA structure. (D) A fit of single-exponential function to the EF-G dissociation kinetics for codon 1 to 7 (translocating into the unstructured region of mRNA). (E) A fit of single-exponential function to the EF-G dissociation kinetics for codon 8 (translocating into the structured region of

mRNA; SL2 mRNA structure is used as shown in fig. S2). **(F)** Average EF-G bound lifetimes with unstructured downstream mRNA region, measured at different temperatures. (n = 378, 212 and 257 molecules from left to right; error bars represent 95% confidence interval for fitting the exponential distribution) **(G)** Average EF-G bound lifetimes with structured and engaged downstream mRNA, measured at different temperatures. (n = 1288, 284 and 105 molecules from left to right; error bars represent 95% confidence interval for fitting the exponential distribution) **(H)** Average EF-G bound lifetimes with structured and engaged downstream mRNA for the last event, measured at different temperatures. (n = 70, 36 and 33 molecules from left to right; error bars represent 95% confidence interval for fitting the exponential distribution) **(I)** Average EF-G bound lifetimes with structured and engaged downstream mRNA on the slippery-sequence. *SL only* is an mRNA construct with the mRNA structure but without any slippery-sequence. *FSPK* mRNA construct has both the mRNA structure and the slippery-sequence. *FSPK_SD* mRNA construct has the mRNA structure, the slippery-sequence, and the upstream Shine-Dalgarno sequence. (n = 1288, 3003 and 565 molecules from left to right; error bars represent 95% confidence interval for fitting the exponential distribution) **(J)** Histogram for tRNA–EF-G FRET efficiencies (black dots) for the condition shown in Fig. 3E, and fitting of the normal distribution (blue curve).

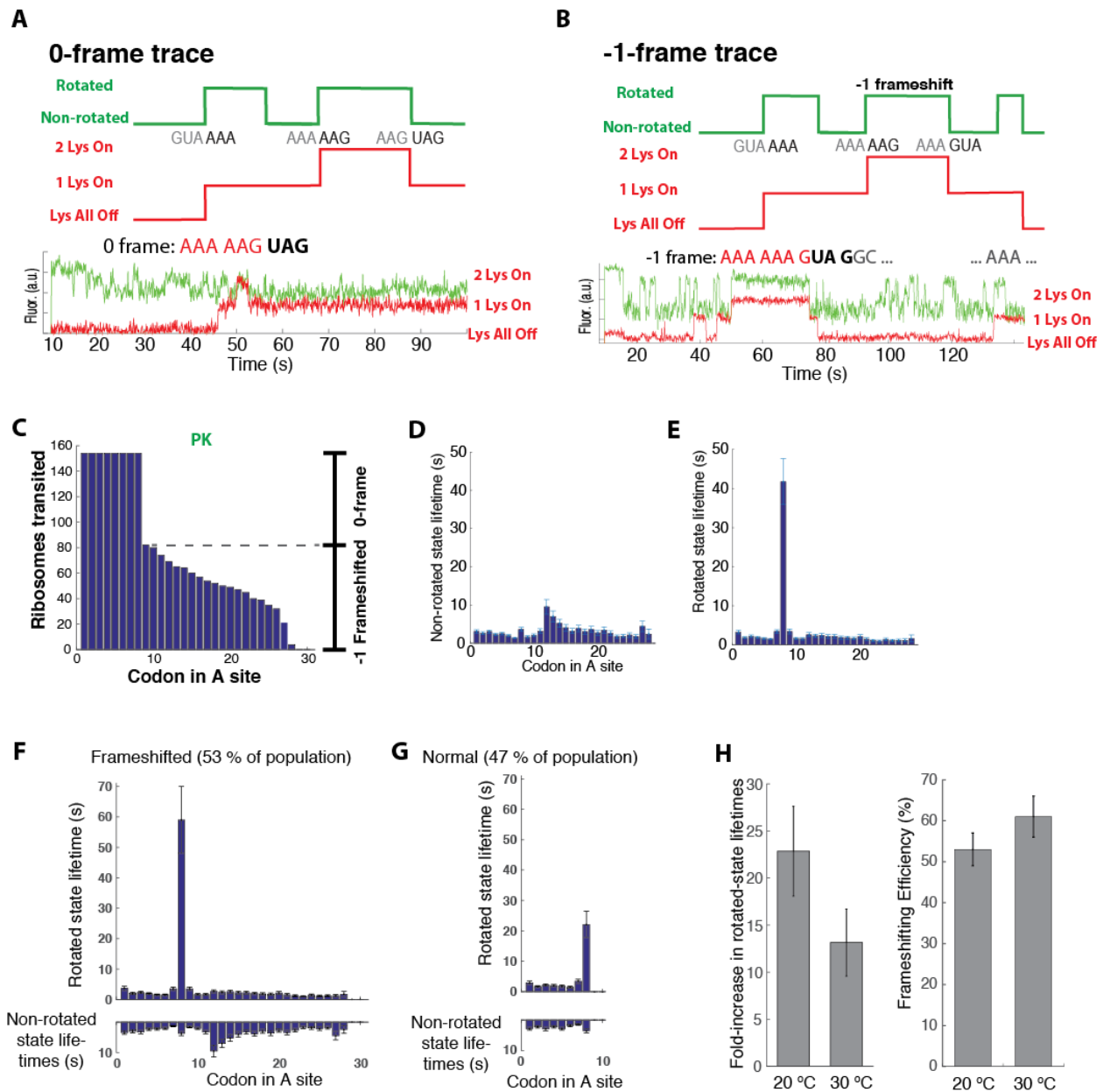


Fig. S3. Assignment of -1 frameshifted population in smFRET assay. (A) Idealized and representative trace of the non-frameshifted ribosome, showing translation arrest at the in-frame stop codon immediately after the slippery-sequence. Translation of slippery-sequence is characterized by two molecules of Cy5-Lys-tRNA bound to the ribosome. Because the termination factors are absent in the in vitro reconstitution system, translation is arrested upon encountering the stop codon in the A site, with P-site tRNA (Cy5-Lys-tRNA) still present. (B) Idealized and representative trace of the frameshifted ribosome, showing continual translation bypassing the in-frame stop codon. (C) A representative ribosome survival (processivity) plot from the mRNA construct containing the slippery sequence and the pseudoknot structure (PK), same as Fig. 4B. (D) A representative non-rotated state lifetime plot from the PK mRNA construct. (E) A representative rotated state lifetime plot from the PK mRNA construct, same as Fig. 4C. (F) Non-rotated and rotated state lifetime plots of the frameshifted population from the PK mRNA construct. (G) Non-rotated and rotated state lifetime plots of the non-frameshifted population from the PK mRNA construct. (H) The fold-increase in rotated-state lifetimes and frameshifting efficiencies (similar to Fig. 4D) for PK constructs measured at two different temperatures ($n = 154$ and 92 for 20 and 30 °C conditions, respectively; error bar representations same as described in Fig. 4D).

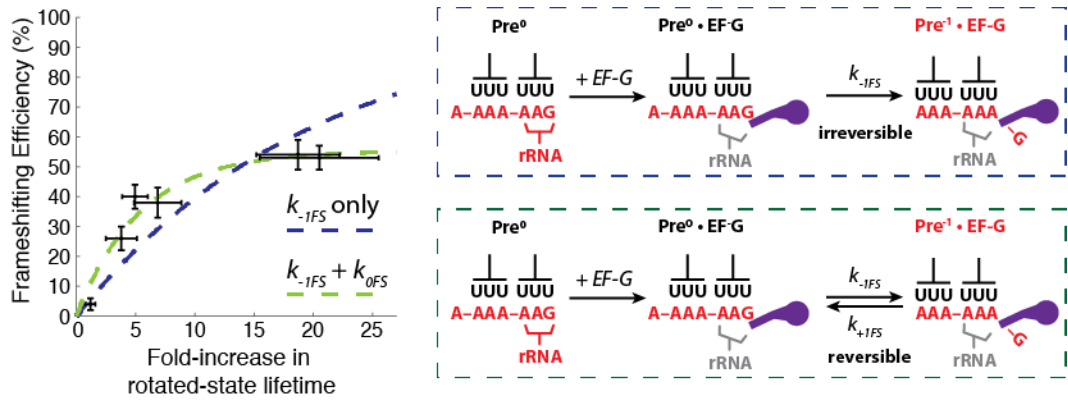


Fig. S4. Simulation of irreversible -1 frameshifting. (Left) A plot of -1 frameshifting efficiency versus the fold-increase in rotated-state lifetimes and two possible models of frameshifting overlaid onto the Fig. 4D. The irreversible model (shown in blue dotted line) has the following fitting statistics: R-squared = 0.63, adjusted R-squared = 0.63, and RMSE = 0.11. The reversible model (shown in the green dotted line) has the following fitting statistics: R-squared = 0.94, adjusted R-squared = 0.93, and RMSE = 0.05. (Right) Two possible models of frameshifting involving either irreversible or reversible frameshifting pathways.

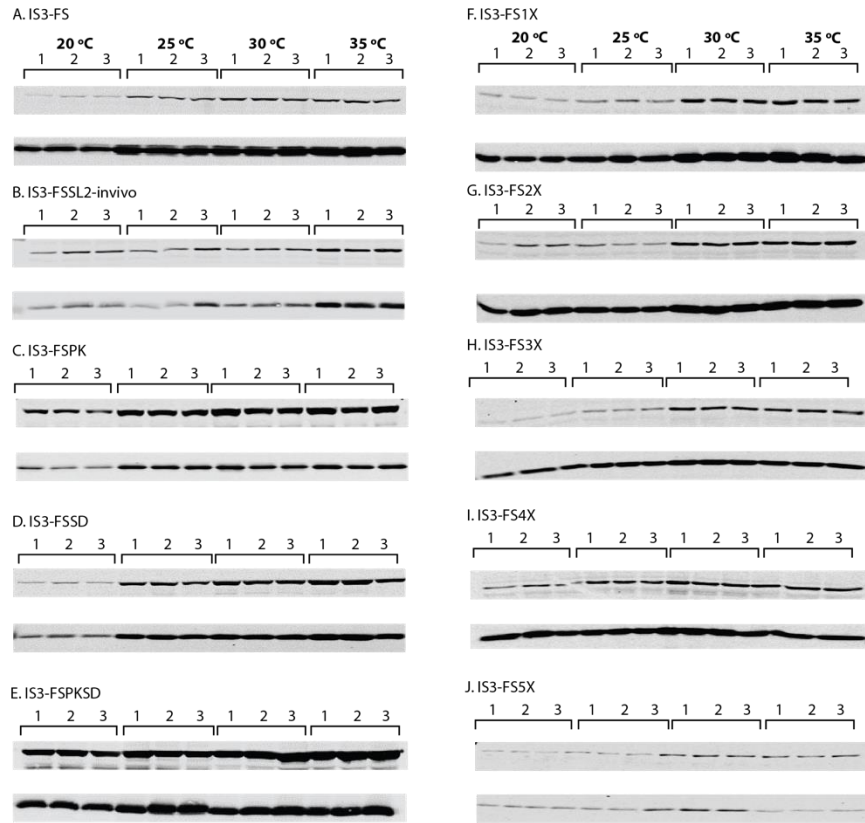


Fig. S5. Western blot gel images for Fig. 5. (A-E) Gel images for Table S1. (F-J) Gel images for Table S2. Each densitometry measurement was made in three technical repeats with varying temperatures (20, 25, 30 and 35 °C; left to right). The upper band shows the production of -1 frameshifted product, whereas the lower band shows the production of the non-frameshifted product.

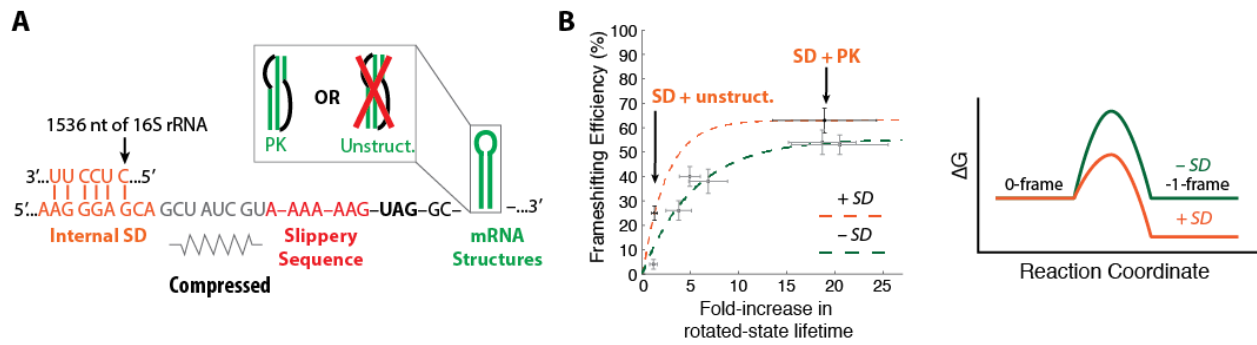


Fig. S6. Internal SD sequence tilts the energy landscape of the frameshifting. (A) mRNA constructs containing the internal Shine-Dalgarno (SD) sequence in addition to the slippery sequence. (B) (Left) Plot of the -1 frameshifting efficiency versus the fold-increase in the rotated-state lifetime of two mRNA constructs containing the internal SD sequence (+ SD), overlaid on the same plot as the Fig. 4D. (Right) The addition of the internal SD sequence may tilt the frameshifting energy landscape. (n = 175 and 75 molecules for unstructured and PK constructs with internal SD sequence; horizontal error bars represent 95% confidence interval after the error propagation; vertical error bars represent standard error from fitting the binomial distribution)

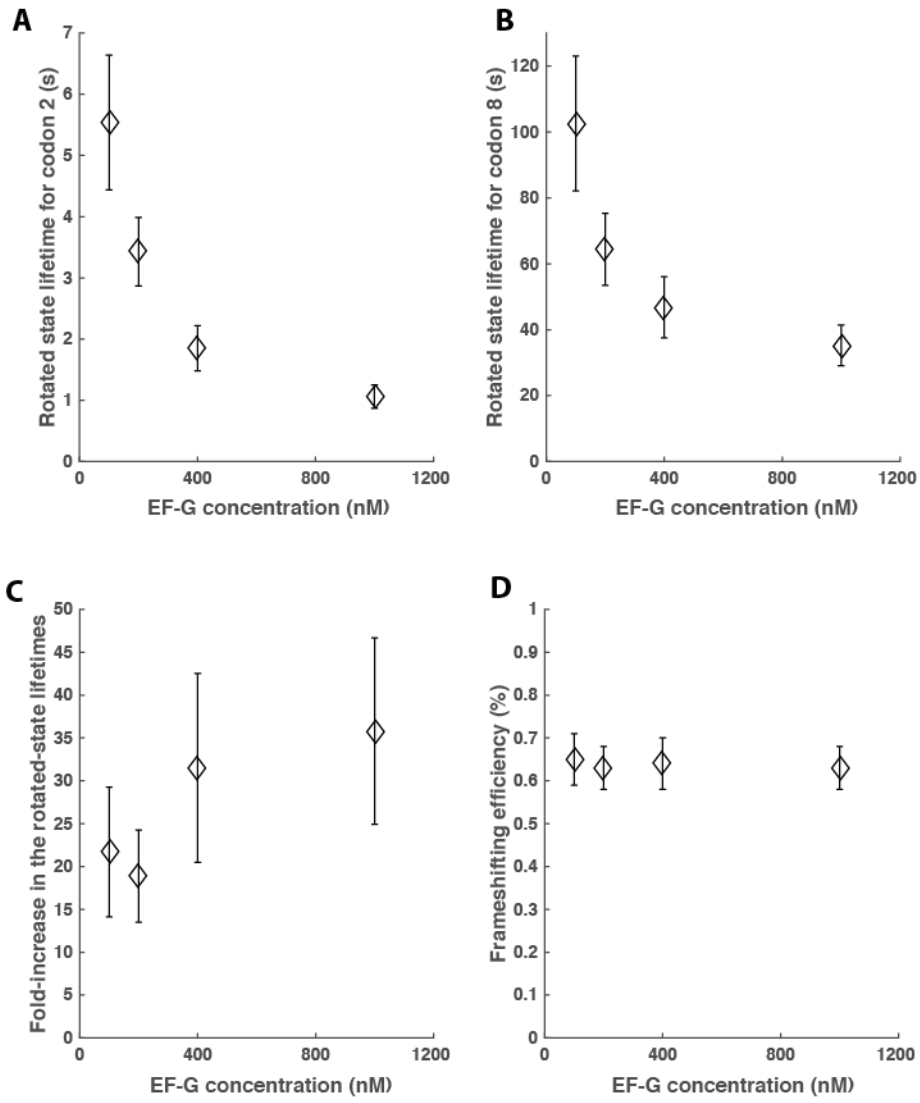


Fig. S7. The concentration of EF-G does not alter frameshifting efficiency. Experiments were performed with IS3-FSPKSD construct (same as used in fig. S6) at varying concentrations of EF-G (100 nM, 200 nM, 400 nM or 1000 nM). **(A)** The rotated state lifetime for codon 2 (Gly). **(B)** The rotated state lifetime for codon 8 (Lys). **(C)** The fold-increase of the rotated state lifetime on the slippery sequence (codon 8). **(D)** Calculated -1 frameshifting efficiency

Table S1. In vivo measurements for frameshifting constructs.

IS3-FS, Frameshifting efficiency (%)					
Temp. (°C)	N1	N2	N3	Std. dev.	Mean
20 °C	6.35	4.46	3.7	1.36	4.84
25 °C	9.36	8	8.09	0.76	8.48
30 °C	9.54	10.69	12.1	1.28	10.78
35 °C	11.26	13.89	13.35	1.39	12.83

IS3-FSSL2-in vivo, Frameshifting efficiency (%)					
Temp. (°C)	N1	N2	N3	Std. dev.	Mean
20 °C	37.43	42.07	45.69	4.14	41.73
25 °C	48.77	44.94	40.83	3.97	44.85
30 °C	38.56	41.60	41.94	1.86	40.70
35 °C	34.99	34.84	38.43	2.03	36.09

IS3-FSPK, Frameshifting efficiency (%)					
Temp. (°C)	N1	N2	N3	Std. dev.	Mean
20 °C	48.95	54.18	44.32	4.94	49.15
25 °C	47.15	45.42	39.15	4.21	43.91
30 °C	49.41	45.00	43.70	2.99	46.04
35 °C	44.50	38.41	44.18	3.43	42.36

IS3-FSSD, Frameshifting efficiency (%)					
Temp. (°C)	N1	N2	N3	Std. dev.	Mean
20 °C	23.94	23.68	19.92	2.25	22.51
25 °C	30.56	29.57	28.56	1.00	29.56
30 °C	34.90	33.98	36.54	1.30	35.14
35 °C	37.09	36.75	34.88	1.19	36.24

IS3-FSPKSD, Frameshifting efficiency (%)					
Temp. (°C)	N1	N2	N3	Std. dev.	Mean
20 °C	51.76	48.28	-	2.46	50.02
25 °C	43.58	38.8	37.77	3.10	40.05
30 °C	47.44	45.92	46.63	0.76	46.66
35 °C	50.39	53.5	48.82	2.38	50.90

Table S2. In vivo measurements for frameshifting on slippery sequence repeat constructs.

IS3-FS1X, Frameshifting efficiency (%)					
Temp. (°C)	N1	N2	N3	Std. dev.	Mean
20 °C	4.36	3.89	4.00	0.25	4.08
25 °C	5.86	5.25	5.85	0.35	5.65
30 °C	10.33	9.97	9.31	0.52	9.87
35 °C	10.20	9.36	9.57	0.43	9.71

IS3-FS2X, Frameshifting efficiency (%)					
Temp. (°C)	N1	N2	N3	Std. dev.	Mean
20 °C	4.19	5.30	4.68	0.55	4.72
25 °C	6.33	7.26	5.47	0.90	6.36
30 °C	11.87	11.01	12.00	0.54	11.62
35 °C	12.44	13.58	17.21	2.49	14.41

IS3-FS3X, Frameshifting efficiency (%)					
Temp. (°C)	N1	N2	N3	Std. dev.	Mean
20 °C	5.20	4.71	4.57	0.33	4.83
25 °C	5.20	4.93	6.22	0.69	5.45
30 °C	12.30	12.31	13.09	0.45	12.57
35 °C	16.01	19.27	16.24	1.82	17.17

IS3-FS4X, Frameshifting efficiency (%)					
Temp. (°C)	N1	N2	N3	Std. dev.	Mean
20 °C	6.40	6.96	6.58	0.28	6.65
25 °C	8.68	9.79	11.61	1.48	10.03
30 °C	18.23	15.55	17.33	1.36	17.04
35 °C	26.60	28.65	25.44	1.63	26.90

IS3-FS5X, Frameshifting efficiency (%)					
Temp. (°C)	N1	N2	N3	Std. dev.	Mean
20 °C	18.70	14.49	9.83	4.44	14.34
25 °C	26.26	19.97	29.88	5.01	25.37
30 °C	31.29	29.30	26.97	2.16	29.19
35 °C	54.87	55.32	57.32	1.30	55.84